Photonically-enabled holographic MIMO with multiple coherently distributed antennas

Shadia Islam Chowdhury[1*], Hannah Sinigaglio[1], Md Saheed Ullah[1], Joseph N. Mait[1], Xiao-Feng Qi[1,2], Shouyuan Shi[1,2], Garrett Schneider[1,2], Janusz A. Murakowski[1,2], and Dennis W. Prather[1,2]

[1]Department of Electrical and Computer Engineering, University of Delaware, Newark, DE 19716, USA
[2]Phase Sensitive Innovations, Inc., Newark, DE 19713, USA

ABSTRACT

We present a photonic-based approach for implementing a coherently distributed antenna system for multiple-input-multiple-output (MIMO) communication at millimeter-wave (mmWave) frequencies. This method utilizes RF-photonic links to enable antenna remoting, ensuring radio frequency (RF) phase coherence over extended distances with minimal loss. Different precoding schemes are applied, and the experimental results are compared with simulation results.

Keywords: MIMO, RF-photonic, mmWave, coherent, distributed antenna, 6G

1. INTRODUCTION

In 6G wireless communication, higher millimeter-wave (mmWave) frequencies play a crucial role due to their multiple GHz bandwidth and increased data rates.[1] However, long-distance transmission at much higher frequencies is impeded by substantial free space path and penetration loss.[2] In wireless communication,[3] system-level performance metrics such as signal-to-noise ratio (SNR), range, and sensitivity can improve overall system performance by employing phased arrays. These arrays enable the steering of one or more beams toward specific objects, either to illuminate them or to enhance signal reception with directional beam gain.

An emerging technique gaining significant interest is holographic MIMO[4–6] which involves the integration of many small and affordable antenna elements across a distributed space, resulting in a spatially distributed or nearly continuous aperture. MIMO technology has developed with time into several subcategories, such as network MIMO,[7] distributed MIMO, cooperative MIMO,[8] coordinated multipoint (CoMP), and others, based on the efficient use of the current equipment and application to certain scenarios. Distributed MIMO systems are increasingly viable for next-generation wireless applications, as multiple antennas are geographically positioned to serve various users simultaneously. This setup achieves significant diversity gain against shadow fading by leveraging independent fading.

A distributed multiuser beamforming architecture is presented here in the optical domain. The optical approach, in contrast to an all-electronic implementation, supports a significantly wider RF spectral range. It also enables the distribution of a common optical local oscillator (LO) signal to remote radio heads located tens of kilometers away. This capability ensures that RF phase coherence is maintained among radio access points (APs) that are geographically distributed.

To enhance the distributed mmWave network,[9] we propose an RF-photonic system that utilizes the photonic generation and distribution of RF signals. This approach leverages high-bandwidth optical components and low-loss optical fiber to enable high-speed, high-frequency microwave communications. It also provides benefits over other applications, such as low-loss transmission, reduced phase noise, lightweight, ultra-wideband operation, distributed coherence, as well as concurrent multi-beam and multi-band performance.[10,11]

This work is funded by Office of Naval Research Grant #N00014-23-1-2742
*E-mail: sharonud@udel.edu

Terahertz, RF, Millimeter, and Submillimeter-Wave Technology and Applications XVIII, edited by Laurence P. Sadwick, Tianxin Yang, Proc. of SPIE Vol. 13365, 1336509 · © 2025 SPIE · 0277-786X · doi: 10.1117/12.3043921

The ability to remotely operate two transmitters over long distances while maintaining mutual phase coherence and minimal signal power loss has been demonstrated, as illustrated in a "Young's Double Slit" experiment using mmWave signals with path length differences of up to 45 kilometers.

This work expands the experiments on coherently distributed beamforming using five transmitters, allowing for adjustable phase and amplitude weights for individual transmit elements. This creates adaptable beam patterns similar to optical holograms, designed to form desired power distributions at appropriate distances.

In this work, we introduce the concept of a photonically enabled coherent distributed antenna system and how this system can be utilized for beamforming at higher frequencies such as mmWave. Experimental results and analysis are presented.

2. RF-PHOTONIC ANTENNA SYSTEM DESIGN

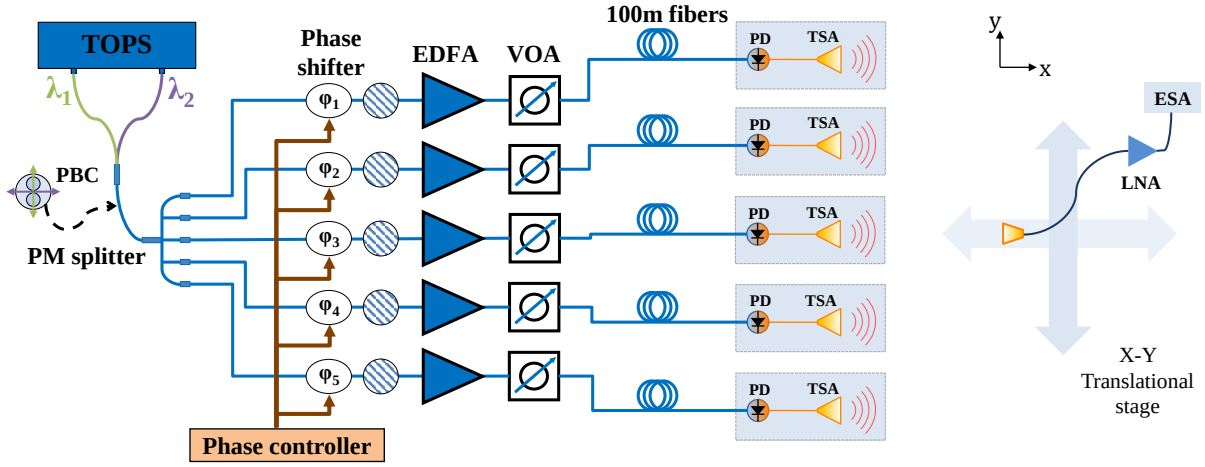

Figure 1: Diagram of an RF-photonic antenna system for a coherent transmitter experimental setup.

Photonically-enabled coherent distributed Tx antennas are illustrated in Fig. 1, where phase coherence is maintained between antennas using an RF-photonic system. By virtue of optical fibers, each antenna can be easily configured in various array formats, in which each channel can be controlled in both amplitude and phase. Using injection-locked lasers,[12] this transmitting array system can generate and transmit high-quality RF signals over long distances. The phase coherence is maintained through a Tunable-Optical paired Source (TOPS),[13] which produces two sinusoidal signals at optical frequencies that are offset by the desired carrier frequency (28 GHz).

The two phase-locked laser signals are combined orthogonally into a polarization-maintaining (PM) fiber using a fiber-based polarization beam combiner (PBC).[14] The PM splitter is then used to divide the combined output into the five-channel feed network.

To regulate the phase, a low-speed lithium-niobate electro-optic phase modulator is applied to each channel to attain a net phase between two optical signals[10] and a linear polarizer is then employed to project them into same polarization. To control amplitude of the signal, variable optical attenuators (VOAs) are employed to each channel. With that, we are able to dynamically adjust both RF phase and amplitude across the antenna array. Each optical signal from the five channels is processed with appropriate complex weighting, similar to a regularized zero-forcing precoding scheme.[15] Afterward, these signals are down-converted and amplified before being transmitted through the antennas. The RF signal is sent using high-power photodetectors (PDs)[16] and conventional antennas, with a high-power PD converting the optical signal into an electrical signal. Multiple transmit antennas work together to focus the signal on the desired location through coherent beam combining.

3. RESULTS

3.1 Experimental Setup

To evaluate the distributed RF phase coherence achieved through the RF-photonic distribution scheme, we deploy an experimental setup as shown in Fig. 2 includes the key components necessary for the coherent distribution of RF signals, such as the TOPS and high-power photodetectors (PDs). This hardware setup is compact, lightweight, cost-effective, and energy-efficient, facilitating analog signal processing. The experimental setup features five tapered slot antennas (TSAs) as transmitters connected to the TOPS via a long fiber link.

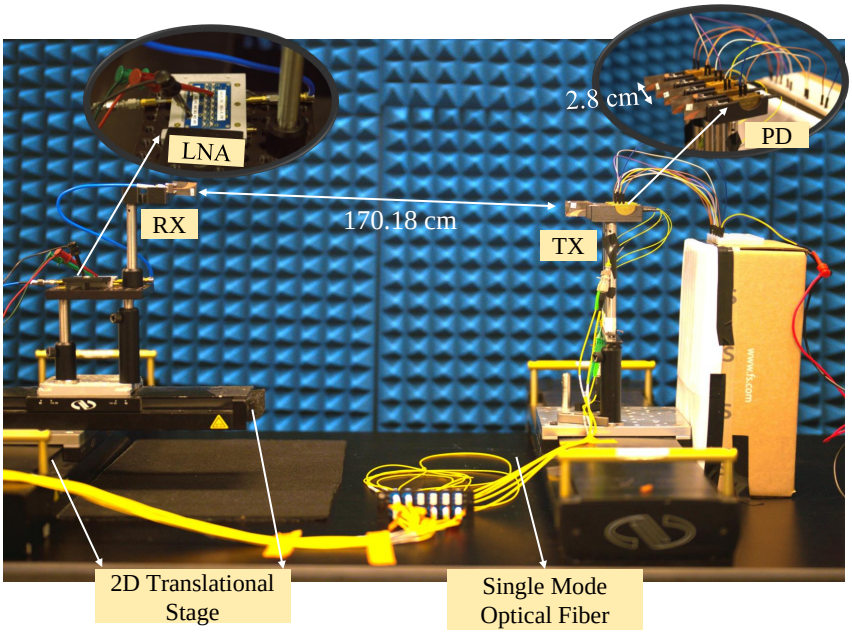

Figure 2: System configuration for assessing performance in experimental analysis.

Currently, all five TSA antenna inputs are connected to high-frequency PDs[16] and they are set up in a linear array with 2.8 cm spacing between each element. Experiments are conducted in an indoor laboratory environment, ensuring a direct line-of-sight (LOS) path between the transmitter and receiver. Simulations are performed using MATLAB with parameters that matches the experimental conditions to ensure consistency. The setup includes five distributed antennas, reflecting the hardware configuration. The spacing between adjacent elements and the distance from the transmit to the receive antenna is set at 2.8 cm and 170.18 cm, respectively, for both simulations and experiments.

To analyze the fringe pattern, both approaches employ a linear translational stage of 60 cm along the axis and operate at a carrier frequency of 28 GHz. The coherent signals emitted by the transmit antenna elements collectively generate a radiation pattern that aligns with the desired in-plane hologram design. An electronic spectrum analyzer (ESA) evaluates the signal power as a TSA receiving antenna, mounted on a linear translational stage, sweeps across RF fringes parallel to the transmit antennas.

Automated control, implemented using LabVIEW, moves the receiving antenna along the stage to identify the peaks and nulls formed by the RF interference pattern. To align the fringe pattern such that a peak or null coincides with the receiving antenna, various phase orientations can be calculated in terms of voltage and applied to the modulator, inducing a phase shift (time delay) at a single output. By precisely adjusting amplitude and phase, an RF in-plane hologram profile is generated, optimizing the far-field radiation pattern to suit the communication system's channel state. This capability extends across a broad operating bandwidth, leveraging photonic components such as electro-optic modulators and optically phase-locked paired signals,[13] enabling efficient RF signal generation and management in the optical domain.

3.2 Performance Analysis

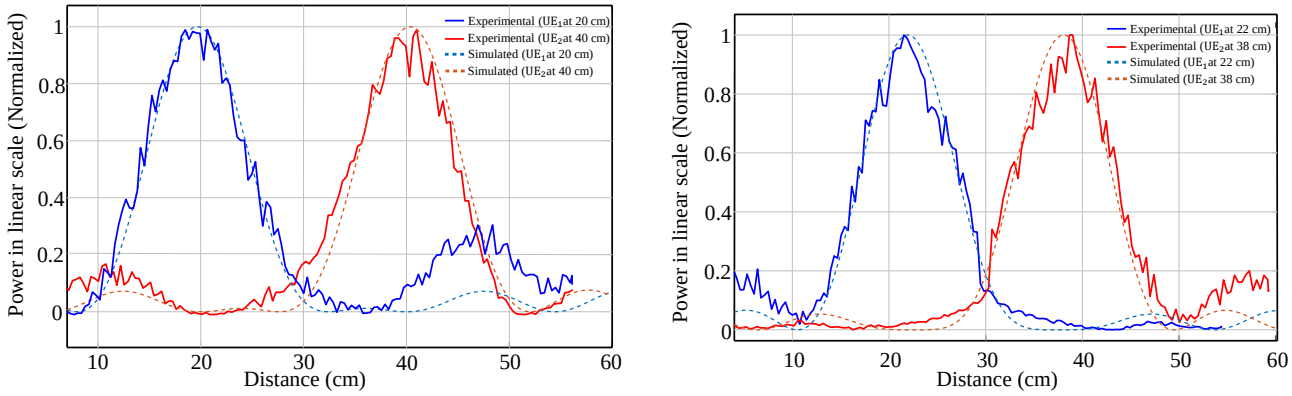

(a) UE_1 at 20 cm and UE_2 at 40 cm

(b) UE_1 at 22 cm and UE_2 at 38 cm

Figure 3: Performance comparison between simulation and lab experiment in terms of fringe pattern.

This presumption corresponds to practical conditions, as the 28 GHz carrier frequency employed in the experimental demonstration is known as the designated frequency bands for 5G communication. In the laboratory, we conduct a performance analysis of the regularized zero-forcing (RZF) precoder[15] for two users, as illustrated in Fig. 3. To visualize the radiation pattern for user equipment 1 (UE_1) and user equipment 2 (UE_2), we activate the optical source (TOPS) one at a time, inputting the calculated complex weighting (phase and amplitude) separately for each user. Specifically, we power one TOPS, apply the complex weighted value, and record the fringe pattern for that user, repeating the process for the second user.

The experimental results, shown in Fig. 3, confirm that the precoder operates as anticipated by the simulations. Additionally, the results illustrate the coherent combination of the five transmitted signals at the user equipment locations, enabling beamforming and steering. Moreover, the findings validate the preservation of phase coherence across widely separated antennas and the effective recovery of the RF carrier after propagating optical signals to the distributed antennas.

Figure 3(a) illustrates the radiation pattern for two users resulting from the beams formed by five distributed antennas. In the system, two users are considered, located at 20 cm and 40 cm along the Y- axis, with their Cartesian coordinates given as $(x, y) = (0,\ 20)$ and $(0,\ 40)$. By maximizing the power at the target user's location while minimizing power at the other user's location, interference can be reduced, leading to an improved signal-to-interference-plus-noise ratio (SINR). The radiation pattern shown in Fig. 3(a) highlights a peak at 20 cm, indicating the power directed towards the target user at that position. A reduction in power leakage from the first user (positioned at 20 cm) to the second user (positioned at 40 cm) is expected to minimize interference.

In Fig. 3(b) two users are positioned at 22 cm and 38 cm along the Y- axis, represented by their Cartesian coordinates $(x, y) = (0,\ 22)$ and $(0,\ 38)$. To minimize the power leakage to the second user, the regularized zero-forcing (RZF) technique creates a null point at the position of User 2 (UE_2).

4. CONCLUSION

We have demonstrated that the distributed RF-photonic phased array antenna system can support one simultaneous user due to limited data encoding units. Our goal is to expand this capability to accommodate multiple simultaneous users. By increasing the number of transmit antennas and applying data modulation to the coherent carriers, we can incorporate multiple users. This will be further demonstrated in future work.

ACKNOWLEDGMENTS

The authors would like to acknowledge to entire team at University of Delaware as well as our collaborators at the Phase Sensitive Innovations.

REFERENCES

[1] Ullah, M. S., Murshed, R. U., Saquib, M., and Uddin, M. F., "Beyond traditional beamforming: Singular vector projection for mu-mimo," *IEEE Communications Letters* (2024).

[2] Ullah, M. S., Sarker, S. C., Ashraf, Z. B., and Uddin, M. F., "Spectral efficiency of multiuser massive mimo-ofdm thz wireless systems with hybrid beamforming under inter-carrier interference," in [*2022 12th International Conference on Electrical and Computer Engineering (ICECE)*], 228–231, IEEE (2022).

[3] Nanzer, J. A., Mghabghab, S. R., Ellison, S. M., and Schlegel, A., "Distributed phased arrays: Challenges and recent advances," *IEEE Transactions on Microwave Theory and Techniques* **69**(11), 4893–4907 (2021).

[4] Prather, D. W., "5g moves into the light: Holographic massive mimo," *IEEEE ComSoc Technology News* (2024).

[5] Wang, Z., Zhang, J., Du, H., Niyato, D., Cui, S., Ai, B., Debbah, M., Letaief, K. B., and Poor, H. V., "A tutorial on extremely large-scale mimo for 6g: Fundamentals, signal processing, and applications," *IEEE Communications Surveys & Tutorials* (2024).

[6] Chowdhury, S., Mait, J., Qi, X.-F., Shi, S., Schneider, G., Prather, D., Murakowski, J., and Schuetz, C., "Two-dimensional radio-frequency holography using distributed apertures," in [*2024 IEEE Conference on Computational Imaging Using Synthetic Apertures (CISA)*], 01–05, IEEE (2024).

[7] Hassan, N. and Fernando, X., "Massive mimo wireless networks: An overview," *Electronics* **6**(3), 63 (2017).

[8] You, X.-H., Wang, D.-M., Sheng, B., Gao, X.-Q., Zhao, X.-S., and Chen, M., "Cooperative distributed antenna systems for mobile communications [coordinated and distributed mimo]," *IEEE Wireless Communications* **17**(3), 35–43 (2010).

[9] Busari, S. A., Huq, K. M. S., Mumtaz, S., Dai, L., and Rodriguez, J., "Millimeter-wave massive mimo communication for future wireless systems: A survey," *IEEE Communications Surveys & Tutorials* **20**(2), 836–869 (2017).

[10] Bai, J., Shi, S., Schneider, G. J., Wilson, J. P., Zhang, Y., Pan, W., and Prather, D. W., "Optically driven ultrawideband phased array with an optical interleaving feed network," *IEEE Antennas and Wireless Propagation Letters* **13**, 47–50 (2013).

[11] Prather, D. W., Galli, S., Schneider, G. J., Shi, S., Murakowski, J. A., Qi, X.-F., and Schuetz, C., "Fourier-optics based opto-electronic architectures for simultaneous multi-band, multi-beam, and wideband transmit and receive phased arrays," *IEEE Access* **11**, 18082–18106 (2023).

[12] Harrity, C., Mahmud, A. A., Schneider, G., Creazzo, T., Murakowski, J., Chester, D., Clyne, K., Mascitelli, T., Schuetz, C., and Prather, D. W., "Tunable optically fed radiofrequency source for distributing coherent high-fidelity signals," in [*2024 IEEE/MTT-S International Microwave Symposium-IMS 2024*], 86–89, IEEE (2024).

[13] Schneider, G. J., Murakowski, J. A., Schuetz, C. A., Shi, S., and Prather, D. W., "Radiofrequency signal-generation system with over seven octaves of continuous tuning," *Nature Photonics* **7**(2), 118–122 (2013).

[14] Schneider, G. J., Murakowski, J. A., Shi, S., Kermalli, M., Galli, S., Qi, X.-F., and Prather, D. W., "Multiuser-mimo transmitter based on optical polar-vector modulators," *IEEE Photonics Technology Letters* **30**(21), 1834–1837 (2018).

[15] Wiesel, A., Eldar, Y. C., and Shamai, S., "Zero-forcing precoding and generalized inverses," *IEEE Transactions on Signal Processing* **56**(9), 4409–4418 (2008).

[16] Beling, A., Xie, X., and Campbell, J. C., "High-power, high-linearity photodiodes," *Optica* **3**(3), 328–338 (2016).